MODELLING COMPLEX DRAFT-TUBE FLOWS USING NEAR-WALL TURBULENCE CLOSURES*

Y. VENTIKOS
Postdoctoral Associate

F. SOTIROPOULOS
Assistant Professor

School of Civil and Environmental Engineering
Georgia Institute of Technology
Atlanta, Georgia 30332, U.S.A.

and

V.C. PATEL
Professor and Director

Iowa Institute of Hydraulic Research
The University of Iowa
Iowa City, Iowa 52242, U.S.A.

Abstract

This paper presents a finite-volume method for simulating flows through complex hydroturbine draft-tube configurations using near-wall turbulence closures. The method employs the artificial-compressibility pressure-velocity coupling approach in conjunction with multigrid acceleration for fast convergence on very fine grids. Calculations are carried out for a draft tube with two downstream piers on a computational mesh consisting of 1.2×10^6 nodes. Comparisons of the computed results with measurements demonstrate the ability of the method to capture most experimental trends with reasonable accuracy. Calculated three-dimensional particle traces reveal very complex flow features in the vicinity of the piers, including horse-shoe and longitudinal vortices and regions of flow reversal.

1. Introduction

Understanding hydroturbine draft-tube flows is a crucial prerequisite for addressing numerous operational and environmental challenges facing the hydropower industry today. From the operational standpoint, the draft-tube is of paramount importance for the overall efficiency and smooth operation of a hydraulic turbine, particularly at off-design conditions. Its importance is best demonstrated by the fact that the primary

---

* To be presented at the *XVIII IAHR Symposium on Hydraulic Machinery and Cavitation*, Valencia, Spain, September 16-19, 1996.

consideration when designing turbine blades is to ensure that they deliver well-conditioned flow at the draft-tube entrance (Fisher, 1995). Poor inflow conditions are associated with several undesirable flow phenomena--flow reversal downstream of the runner, formation of rope vortices, and cavitation--which could induce large efficiency losses, devastating pressure pulsations in the entire system, and even failure. From the environmental standpoint, draft tube flows are important for understanding the causes of injury and/or mortality of passing fish as well as for developing effective strategies for improving the tailrace water quality. Regions of large flow gradients, intense streamwise vortices, cavitation, areas of flow recirculation, and formation of the so-called "back-roll" vortices at the draft-tube/tailrace interface may be responsible for injuring and/or disorienting passing fish. On the other hand, tailrace water quality, which is affected by the depletion of Dissolved Oxygen (DO) in the lower levels of the reservoir during warm months of the year (Bohac and Ruane, 1991), may be substantially improved using autoventing hydroturbines (AVT). AVT technology relies on turbulence mixing within the draft tube to ensure transfer of oxygen from the air-bubbles--injected into the water at strategic locations downstream of the runner--to the water at a rate sufficient to increase the tailwater DO concentration at environmentally acceptable levels (Carter, 1995).

A typical draft tube consists of a short conical diffuser followed by a strongly curved 90^{o} elbow of varying cross-section and then a rectangular diffuser section. Its cross-sectional shape changes continuously from circular at the inlet, to elliptical within the elbow, and finally to rectangular at the exit. Additional geometrical complexities include the presence of one or more piers, downstream of the elbow, splitter blades, guide vanes, slots, etc. The flow that enters the draft tube--the wake of the turbine runner--is turbulent and three dimensional, with high swirl levels. This already complex inlet flow undergoes additional straining as it passes through the elbow, induced by the rapid area changes, the very strong longitudinal curvature, and the presence of various obstacles. The resulting flow is extremely complicated with regions of strong induced pressure gradients, intense longitudinal and horse-shoe vortices, regions of flow reversal, etc. These complexities make the numerical simulation of draft tube flows particularly challenging for even the most advanced numerical methods available today. Yet modern computational fluid dynamics (CFD) methods offer the most promising alternative for elucidating the physics of draft tube flows at a level of detail necessary for addressing the operational and environmental issues noted above.

Numerical simulations of draft tube flows have been reported, among others, by Vu and Shyy (1988), Agouzoul et al. (1990), Sotiropoulos and Patel (1993), and Reidelbauch et al. (1995). With the exception of Sotiropoulos and Patel (1993)--who employed a two-layer near-wall k-ε model and a moderately fine computational mesh (approximately 200,000 nodes)--all these studies adopted the standard, high Reynolds number, k-ε model with wall functions, and reported results on rather coarse meshes (40,000 to 100,000 nodes). Despite reproducing general physical trends, regarding the effect of inflow swirl on the flow development, none of these studies demonstrated their ability to quantitatively predict the flow details.

The objective of this work is to develop the computational framework that would enable accurate quantitative predictions of turbulent flows through complex draft-tube geometries over a range of operating conditions. An efficient, finite-volume numerical method is presented for solving the three-dimensional Reynolds-averaged

DISCLAIMER

DISCLAIMER

Portions of this document may be illegible electronic image products. Images are produced from the best available original document.

Navier-Stokes equations in conjunction with near-wall turbulence closures on very fine, highly stretched and skewed computational meshes. Numerical solutions are obtained for one of the Norris Power Plant draft tubes (Tennessee Valley Authority) at model-scale Reynolds numbers. The two-layer k-ε model of Chen and Patel (1988) is employed for turbulence closure. The computed solutions are compared with available mean velocity measurements at several locations downstream of the elbow (Hopping, 1992) and analyzed in terms of three-dimensional particle traces.

2. The numerical method

The numerical method of Sotiropoulos and Lin (1996) is modified and used in the present study. This method solves the three-dimensional Reynolds-averaged Navier-Stokes (RANS) equations, in conjunction with two-equation, near-wall, turbulence closures, formulated in generalized curvilinear coordinates in strong conservation form. Pressure-velocity coupling is achieved using the artificial compressibility approach. The governing equations are discretized on a non-staggered computational mesh using finite-volume discretization schemes. Three-point central differencing is employed for the viscous fluxes and source terms in the turbulence closure equations. The method features a number of options for approximating the spatial derivatives of the convective flux-vectors. These include second-order, central--with scalar and matrix valued fourth-difference artificial dissipation terms--and flux-difference splitting upwind (ranging from first to fifth-order accuracy) differencing schemes. The spatial resolution of these schemes has been carefully evaluated in both laminar (Lin and Sotiropoulos, 1996a) and turbulent flow simulations (Sotiropoulos and Lin, 1996b).

The discrete mean flow and turbulence closure equations are integrated in time using a four-stage explicit Runge-Kutta algorithm (Jameson, 1983) enhanced with local time-stepping, implicit residual smoothing, and multigrid acceleration. A three-grid level V-cycle algorithm with semi-coarsening in the transverse plane (that is, coarse grids are constructed by doubling the grid spacing only in the transverse directions) is employed in the present study. One, two, and three iterations are performed on the first, second, and third grid level, respectively. The present multigrid method is capable of solving the turbulence closure equations in both loosely and strongly-coupled fashion. In the first approach, multigrid is applied only to the mean-flow equations while the turbulence closure equations are solved only on the finest mesh (the eddy-viscosity values are injected to the coarser meshes and held constant during the cycling process). In a strongly coupled strategy, on the other hand, multigrid is applied simultaneously to both the mean and turbulence closure equations and the eddy-viscosity values are updated at each grid level (see Sotiropoulos and Lin (1996) for a detailed discussion and comparison of the various methods). All subsequently presented calculations have been obtained using the loosely coupled algorithm with three iterations performed on the turbulence closure equations per multigrid cycle.

The present method features a number of isotropic and non-isotropic (non-linear) two-equation turbulence models (see Sotiropoulos and Ventikos (1996) for details). In the present study, however, only the isotropic two-layer k-ε model of Chen and Patel (1988) is employed. Work is currently underway to implement and validate the various non-linear models for draft-tube geometries.

3. Test case and computational details

The draft tube configuration, used for the present computations, is one of the TVA Norris Autoventing Power Plant (Norris, Tennessee) draft tubes designed to operate with 66.000 HP hydroturbines. The area expansion ratio for this draft tube (ratio of the exit to inlet cross-sectional area) is approximately 4.4:1 while the radius of curvature of the elbow is 1.34 diameters of the inlet circular cross-section. Two vertical piers, symmetrically placed about the centerline, support the downstream rectangular diffuser.

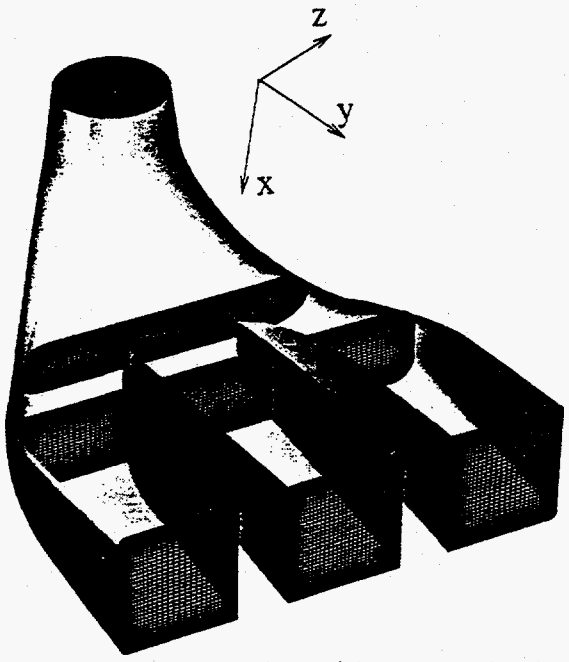

Figure 1. Cross-sectional views of the computational grid

The computational grid for every cross-section is generated using an efficient algebraic grid generation method which employs linear and third-order spline interpolation. The grid lines are concentrated near the walls using the hyperbolic tangent stretching function. The cross-sectional grids are then stacked along the centerline of the tube to complete the three-dimensional grid. To accurately resolve the flow in the vicinity of the piers, the streamwise planes are clustered around the pier leading edges also using hyperbolic tangent stretching. Typical cross-sectional views of the computational mesh and the relevant coordinates are shown in figure 1. All the subsequently reported calculations were carried out on a grid with 85 x 73 x 193 nodes (a total of approximately 1.2×10^6 nodes), in the streamwise, vertical, and horizontal (ξ, η, and ζ) directions, respectively, which is the finest mesh to be used so far for draft-tube calculations. The near-wall coordinate surfaces are located everywhere such that $1 < n^+ < 5$, where $n^+ = u_\tau n/\nu$ (u_τ is the shear velocity, n denotes the distance from the wall, and ν is the molecular kinematic viscosity).

Inlet conditions are specified using the experimental measurements (Hopping, 1992). These include both the axial and transverse mean velocity components at a plane downstream of the runner (see Figure 2). The measurements were carried out using a laser velocimeter for a range of operating conditions with and without air injection. The present simulations correspond to experimental run No. 1 (see Hopping, 1992) which was performed with the air off, runner speed 898 rpm, net head 24.8m, and water discharge 0.44cm^3/sec. These conditions correspond to a Reynolds number Re=1.1x10^6, based on the diameter D, and bulk velocity U_b at the inlet of the draft tube. It should be noted that inlet measurements were obtained along two mutually perpendicular radii (see Figs. 2a, and c), which suggest that the flow is not circumferentially symmetric. Due to lack of more detailed data, however, the calculations were carried out by arbitrarily choosing one of the two profiles and assuming that the inlet flow is axisymmetric. To facilitate the application of outflow boundary conditions, an artificial straight extension (of total length 10D) was added downstream the end of the draft tube. The flow quantities at the downstream end of this extension were obtained by assuming zero streamwise diffusion. On the solid walls the velocity components and turbulence kinetic energy are set equal to zero. The pressure at all boundaries is calculated by using linear extrapolation form the interior nodes.

The computational domain is treated as a single block with the piers accounted for by using a blanking technique. This treatment necessitates the use of several two-dimensional arrays to store the Jacobian and metrics of the geometric transformation and the pressure field on each pier wall. Converged solutions (four orders of magnitude reduction in residuals) are obtained after approximately 800 multigrid cycles. The computational time per grid node per cycle is 2.2x10^{-4} secs on a single-processor Silicon Graphics, 90MHZ, R8000, Power Challenge workstation.

4. Results and Discussion

In this section we present comparisons of calculated mean streamwise velocity profiles with measurements at several locations within the three bays. The numerical solutions are also interrogated using particles traces to elucidate the structure of the three-dimensional flow separation and vortex formation phenomena within the elbow and the downstream diffuser.

Figure 2 shows comparisons of measured (Hopping, 1992) and calculated streamwise mean velocity profiles at two streamwise locations, downstream the start of the piers, in all three bays. The velocity profiles, are plotted at two y = constant planes (see Figures 2a and 2c for axes definition) along the horizontal (Fig. 2a), and vertical (Figs. 2b, c, and d) centerlines of each cross-section. Figures 2a and 2c also include the measured streamwise and swirl velocity components at the inlet section, which, as discussed above, were used to provide inlet conditions for the calculations. All velocities in these figures have been scaled by the bulk velocity at the inlet of the draft tube.

The measurements in Fig. 2 suggest that most of the flow passes through the left (with respect to an observer standing at the draft-tube inlet looking downstream) bay. This is evident by the overall larger velocities through that bay and is obviously associated with the clockwise direction of the inflow swirl. The calculations reproduce this flow feature and appear to capture reasonably well most experimental trends. Some

discrepancies are observed at the downstream location in the right bay (Fig. 2a), where the calculated streamwise velocity profile indicates the presence of a small reversed flow

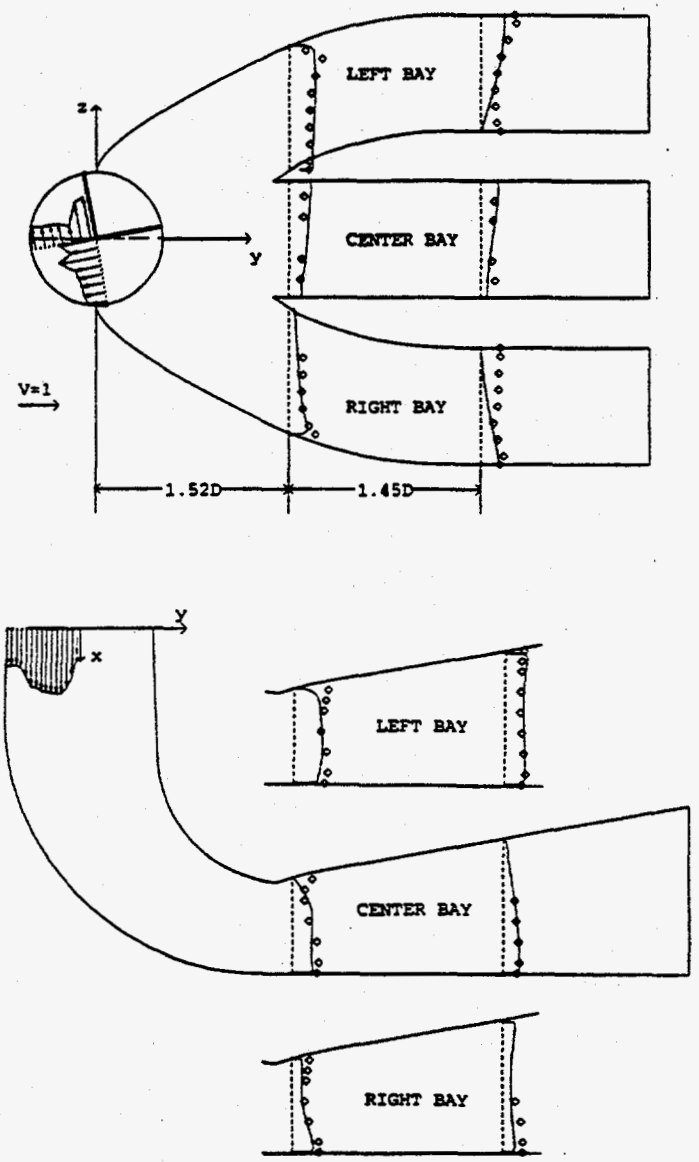

Figure 2. Comparisons of measured and computed streamwise mean velocity profiles

region near the inner wall. Contour plots of the calculated streamwise velocity component, not shown here due to space considerations, reveal a recirculating flow region starting upstream of that section and ending immediately downstream. The measurements, on the other hand, suggest a fuller and almost uniform velocity profile there which appears to have recovered very rapidly from its upstream distorted shape. Similar discrepancies, albeit not as pronounced, are observed at the downstream section in the left bay as well. It should be noted, however, that the experimental measurements are not detailed enough to allow a comprehensive assessment of the accuracy of the numerical solutions. Given the continuous area expansion downstream of the elbow, it is very likely that reversed flow does exist in the experiment, although may be not at the same locations indicated by the calculations, but could not be resolved by the few available velocity measurements. Yet another source of uncertainty is the lack of detailed velocity measurements at the inlet. As discussed in the previous section, the inlet flow was assumed axisymmetric, although the limited available measurements do not support such an assumption (see inlet swirl profile in Fig. 2a). Given the complexity of the draft-tube geometry, even small differences in inlet conditions could account for the observed discrepancies. Obviously, the present calculations can not offer positive answers to all these questions. They do, however, underscore the need for carefully designed, very detailed laboratory experiments.

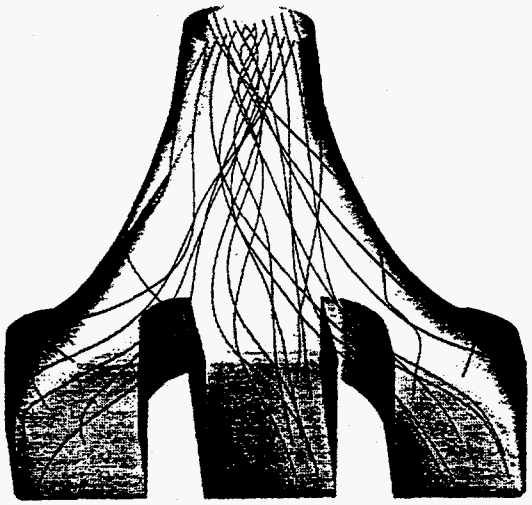

Figure 3. Three-dimensional particle traces: General view

Figures 3, 4 and 5 depict particle traces released at strategically selected locations to clarify various three-dimensional flow features. A global view of the flowfield is given in Fig. 3, which shows the paths of particles originating along two mutually perpendicular diameters at the inlet plane. It is seen that most of the flow passes through the left bay and the left half of the center bay, which is consistent with the trends exhibited by the velocity profiles discussed above. Particles released near the center of the inlet section are seen to form a coherent, rope-like, vortical structure which appears to pass through the left half of center bay. Significant secondary motion is also

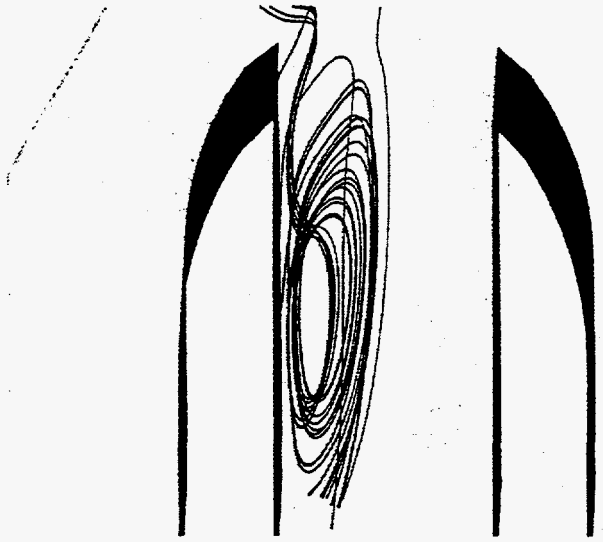

Figure 4. Three-dimensional particle traces: Reversed flow region

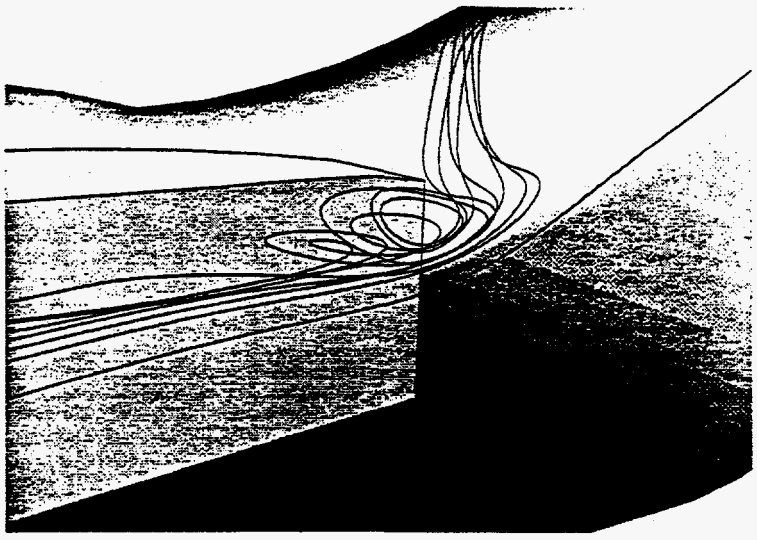

Figure 5. Three-dimensional particle traces: Horse-shoe vortex

present in the right bay as indicated by the twisting particle trajectories there. Figures 4 and 5 reveal some very complex three-dimensional flow patterns along the flat wall of the right pier. Figure 4 indicates the existence of a recirculation region which is located

near the top (diverging) wall of the draft tube--although not shown herein due to space limitations, the particles that are trapped in this area originate from the near-wall region at the left side of the inlet section. Underneath this recirculating flow region there is a very intense longitudinal vortical structure which is shown in Figure 5. This structure is similar to horse-shoe like vortices known to form at wing-body junctions and is produced by lateral skewing of the vorticity vector. These flow patterns--which to the best of our knowledge have not been reproduced before numerically for draft-tube geometries--serve to demonstrate the enormous complexities of such flows, underscore the challenges for advanced CFD methods, and point, once again, to the need for very detailed laboratory experiments to provide data for numerical validation.

5. Summary and Conclusions

An efficient finite-volume method was presented for carrying out fine-grid calculations with near-wall turbulence models for complex draft-tube geometries. The computed solutions are compared with mean velocity measurements downstream of the elbow. The calculations reproduce most experimental trends with reasonable accuracy. Three-dimensional particle traces reveal, for the first time, the presence of very complex three-dimensional flow patterns around the piers. These include longitudinal and horse-shoe vortex formation, and regions of reversed flow. The present study underscores that detailed three-dimensional flow measurements are of crucial importance for further advancements in numerical modelling of real-life draft-tube geometries. Current work focuses on further improving the efficiency of the multigrid method, by implementing grid sequencing techniques, as well as implementation and testing of advanced turbulence models that account for turbulence anisotropy.

6. Acknowledgments

The initial phase of this work, while the second author was at the University of Iowa, was supported by a grant from the Tennessee Valley Authority. The continuation of this work at the Georgia Institute of Technology is funded by Voith Hydro, Inc. and the U.S. Department of Energy. The authors are most grateful to Richard K. Fisher, Jr., of Voith Hydro, Inc., and Patrick March and Paul Hopping, of TVA, for their advice and support.

7. References

Agouzoul, M., Reggio, M., and Camarero, R. (1990), "Calculation of Turbulent Flows in a Hydraulic Turbine Draft Tube," *ASME J. Fluids Eng.*, 112, pp. 257-263.

Bohac, C. E., and Ruane, RT. J. (1991) "Tailwater Concerns and the History of Turbine Aeration," ASCE National Hydraulic Engineering Conference.

Carter, J., Jr. (1995) "Recent Experience with Turbine Venting at TVA," *Water-Power 95*, ASCE Int. Conf. & Exposition on Hydropower, San Francisco, California, Vol. 2, pp. 1396-1405.

Chen, H. C. and Patel, V. C. (1988), "Near-Wall Turbulence Models for Complex Flows Including ," *AIAA J.*, Vol. 26, pp. 641-648.

Fisher, Jr., R. K. (1995), private communication.

Hopping, P. N. (1992), "Draft Tube Measurements of Water Velocity and Air Concentration in the 1:11.71 Scale Model of the Hydroturbines for Norris Dam," *Tennessee Valley Authority Engineering Laboratory*, Report No. WR28-2-2-116, Norris, Tennessee.

Jameson, A. (1983), "Solution of the Euler Equations by a Multigrid Method," *Applied Mathematics and Computation*, Vol. 13, pp. 327-356.

Lin, F., and Sotiropoulos, F. (1996a), "Assessment of Artificial Dissipation Models for Three-Dimensional, Incompressible Flow Solutions," to appear in the *ASME J. of Fluids Engineering* (April 1995).

Lin, F., and Sotiropoulos, F. (1996b), "Strongly-Coupled Multigrid method for 3-D Incompressible Flows Using Near-Wall Turbulence Closures," to appear in the *ASME J. of Fluids Engineering*.

Riedelbauch, S., Fisher, Jr., R. K., Faigle, P., and Franke, G. (1995), "The Numerical Laboratory Gets Better," *Water-Power 95*, ASCE Int. Conf. & Exposition on Hydropower, San Francisco, California, pp. 1386-1395.

Sotiropoulos, F., and Patel, V. C. (1992), "Flow In Curved Ducts Of Varying Cross-Section," Iowa Institute of Hydraulics Research, IIHR report No. 358, The University of Iowa, Iowa City, Iowa.

Sotiropoulos, F., and Ventikos, Y. (1996), "Assessment of Some Non-Linear Two-Equation Turbulence Models in a Complex, 3-D, Shear Flow," to be presented at and appear in the proceedings of the *6th International Symposium on Flow Modelling and Turbulence Measurements*, September 8-10, Tallahassee, Florida.

Shyy, W. and Braaten, M. E., (1986), "Three-dimensional Analysis of the Flow in a Curved Hydraulic Turbine Draft Tube," *Int. J. Numerical Methods in Fluids*, Vol. 6, pp. 861-882.

Vu, T. C. and Shyy, W. (1990), "Viscous Flow Analysis as a Design Tool for Hydraulic Turbine Components," *ASME J. Fluids Engineering*, Vol. 112, pp. 5-11.